The Alpha 4 Nicotinic Receptor Promotes CD4+ T-Cell Proliferation and a Th2 Immune Response

Jacob C. Nordman, Pretal Muldoon, Sarah Clark , M. Imad Damaj, Nadine Kabbani

Department of Molecular Neuroscience, Krasnow Institute for Advanced Study, George Mason University, Fairfax, Virginia 22030 (JCN, SC, NK). Department of Pharmacology and Toxicology, Virginia Commonwealth University, Richmond, VA 23298 (PM, MID).

1

*Running Title: Alpha 4 Promotes CD4 Proliferation

To whom correspondence should be addressed: Nadine Kabbani, Department of Molecular
Neuroscience, Krasnow Institute For Advanced Study, George Mason University, 4400
University Drive, Fairfax, VA 22030, Tel.: (703) 993-4406, Fax.: (703) 993-4325; E-mail:
nkabbani@gmu.edu

Text page #: 37

Table #: 0

Figure #: 8

References #: 60

Abstract word #: 152

Introduction word #: 454

Discussion word #: 820

Abbreviations: Th, T-helper; CD, cluster of differentiation; $G\alpha_o$, G protein subunit o; nAChR, nicotinic acetylcholine receptor; Gprin1, G protein regulated-inducer of neurite outgrowth; OSHA, occupational safety and health administration; ICF, immune cell fraction; BMF, bone marrow fraction; Ab, antibody; Nic, nicotine; MSP, mastoparan; NK, natural killer cell; DHβE, dihydro-beta-erythroidine; ACh, acetylcholine; LC-ESI, liquid chromatograph electrospray ionization; MS, mass spectrometry.

ABSTRACT

Smoking is a common addiction and a leading cause of disease. Chronic nicotine exposure is known to activate nicotinic acetylcholine receptors (nAChRs) in immune cells. We demonstrate a novel role for α4 nAChRs in the effect of nicotine on T-cell proliferation and immunity. Using cell based sorting and proteomic analysis we define an α4 nAChR expressing helper T-cell population (α4+CD3+CD4+) and show that this group of cells is responsive to sustained nicotine exposure. In circulation, spleen, and thymus we find that nicotine promotes an increase in CD3+CD4+ cells via its activation of the α4 nAChR and regulation of $G\alpha_o$, Gprin1, and CDC42 signaling within T-cells. In particular, nicotine is found to promote a Th2, adaptive, immunological response within T-cells, which was absent in α4-/- mice. We thus present a new mechanism of α4 nAChR signaling and immune regulation in T-cells, possibly accounting for the effect of smoking on the immune system.

INTRODUCTION

Smoking is one of the most prevalent addictions and comes replete with numerous health risks.

Among these, smoking has been implicated as a causative agent for various disorders including

most cancers, cardiovascular disease, and autoimmune diseases such as lupus and myasthenia

gravis (Costenbader and Karlson, 2005; Moreau et al., 1994). Nicotine appears to target

lymphatic organs such as the spleen, thymus, and lymph nodes and has been shown to play a role

in bacterial immunity (Andersson, 2005), increased IL-6 production in spleen (Song et al., 1999),

and T-cell maturation (Middlebrook et al., 2002). Recent studies show a connection between

cigarette smoke and the helper T-cell (Th) driven Th1/Th2 division of immunity in which

smoking promotes Th2 related adaptive immunological responses (Zhang and Petro, 1996).

The molecular target of nicotine is a class of ligand-gated ion channels also activated by

the endogenous neurotransmitter acetylcholine (ACh) (Changeux, 2010). In mammals, 17

subunits (α1– α7, α9, α10, β1– β4, γ, δ, ϵ) confer the expression of a functional nicotinic

acetylcholine receptor (nAChR) in cells (Changeux, 2010). A subset of nAChRs have been

discovered in immune cells (Kawashima and Fujii, 2003) however to date a nicotinic activated

current has not been detected in lymphocytes. Clearly however a number of systems, including

the neural immune "inflammatory reflex", depend upon the activity of nAChRs. For example,

cytokine-producing macrophages in the spleen contain α7 nAChRs, which regulate the activity

of the vagus nerve (Rosas-Ballina et al., 2011). α7 nAChR agonists, including nicotine, appear to

regulate cytokine production in immune cells of the lung and spleen suggesting that nAChRs

present a possible new drug target for inflammatory disease.

α4 subunits are amongst the most common nAChRs contributing to the formation of the

high-affinity (α4β2) nicotine-binding site in cells (Changeux, 2010). In mice lacking the α4

nAChR (α4-/-) nicotine binding appears to be all but abolished in several organs (Marubio et al., 1999). α4 nAChRs are well expressed in immune cells including T- and B-lymphocytes and have been implicated in regulating cytokine release as well as antibody production (Skok et al., 2007). Indeed α4-/- mice have been found to exhibit abnormalities in lymphocyte development and maturation (Skok et al., 2007). Because exposure to nicotine appears to up-regulate α4 containing nAChRs in lymphocytes of human smokers and in rodents (Cormier et al., 2004) we hypothesize an effect of nicotine on immunity. In this study we show the existence of an α4 nAChR expressing population of T-lymphocytes (α4+CD3+CD4+) in circulation, spleen, bone marrow, and thymus. We demonstrate that nicotine enhances the number of α4+ T-cells in these immune organs leading to a change in cytokine production and release. This mechanism is driven by α4 nAChR signaling via a G protein/CDC42 pathway in T-cells.

MATERIALS AND METHODS

Animals

C57BL6 adult male mice were kept in 12-hour light/dark cycles. The generation of α4 nAChR subunit knockout (α4-/-) mice was previously described (Ross et al., 2000). For all experiments, α4-/- mice were backcrossed to at least 10-12 generations. α4-/- and wild-type (WT) mice were obtained from crossing heterozygote mice.

Isolation of the immune cell fraction

An immune cell fraction (ICF) from blood was obtained from the heart via cardiac puncture (Hoff, 2000) and from the spleen and thymus through dissection according to Institutional Animal Care and Use Committee (IACUC) regulations. Mice were anesthetized using 5% isofluorane and the heart, thymus, and spleen were accessed via an abdomen to sternum incision. For circulating heart blood (ICF$_C$), a 1cc syringe with a 25½ gauge needle was inserted into the left ventricle and blood was drawn to a volume of 500 μl/mouse. Equal volumes of phosphate buffered saline (PBS) with 5mM EDTA (PBSE) was added to the blood fraction as an anti-coagulant. Bone marrow fractions (BMF) were obtained by removing the hind leg bones (femur and tibia) and an opening was made to expose the bone marrow. The bone marrow was aspirated out using 0.075M KCl and then incubated at 37°C for 15 min prior to centrifugation at 800 x g to collect the BMF. Tissue dissected from the spleen and thymus was weighed then homogenized by manual trituration using a sterile Pasteur pipette. The supernatant was centrifuged at 250 x g and the pellet resuspended in PBSE. Circulating, spleen, and thymus ICF were isolated and pooled using Ficoll-Paque (GE Healthcare) per manufacturer instructions.

6

Immune bead sorting assay

Immune cells were isolated using a magnetic bead method based on the protocols of (Zhichao et al., 2000) with modification. For cell isolation, ICF was preincubated with 10 μg rat monoclonal anti-α4 Ab (mAb299) (Whiting and Lindstrom, 1988), mouse polyclonal anti-CD4 Ab (SC), or rabbit IgG Abs (Cell Signaling) in ice-cold PBS for 2 hours prior to the addition of a pre-cleared Protein-G Dynabead resin (Life Sciences). Cells were incubated with the beads for 1 hour and then eluted from the bead matrix by gentle mixing in a 5 μg/ml papain in PBS solution for 15min at room temp. Papain was inactivated by the addition of RPMI culture media with 5% FBS followed by washing in PBS and slow speed centrifugation (100 x *g*).

Fluorescence activated cell sorting

Fluorescence activated cell sorting (FACS) was conducted using a published protocol (Yoder et al., 2008) with minor modifications. Briefly 1-2x10^6 immune cells were pelleted, fixed and probed with 5 μg mAb299 and FITC conjugated CD4 (BD Biosciences) for 30 minutes in the dark. Secondary staining was conducted using Dylight 488 (Pierce) for 30 min in the dark. Cells were washed with PBS then resuspended in a 1% paraformaldehyde fixative prior to analysis using a FACSCalibur (Becton Dickinson).

Drug treatments

WT and α4-/- mice were given a sustained (6-day) regimen of 0.9% saline or nicotine dissolved in 0.9% saline (0.1-1.5 mg/kg body weight) intraperitoneal injections. Injections were normalized to equal volume solutions made fresh daily. Nicotine concentrations were based on published studies on chronic drug associated behaviors (Marubio et al., 2003) and immune effect

7

(Davis et al., 2009). Unless otherwise noted, sustained nicotine treatment is a 6-day treatment.

For cell culture experiments, CEMss cells were exposed to nicotine, nicotine and DHβE,

Mastoporan (MSP), or MSP and nicotine as in (Amin et al., 2003; Nordman and Kabbani, 2012).

Immunocyctochemistry and Cell Counting

Cells derived from ICF and CEMss cells were fixed for 15 min at room temp using a solution

consisting of 1 x PEM (80 mM PIPES, 5 mM EGTA, and 1 mM MgCl2, pH 6.8) containing

0.3 % glutaraldehyde. Cell were centrifuged at 1000 x *g* for 5 min then washed with PBS. For

Gprin1 staining, cells were permeabilized with 0.1% Triton X-100 prior to glutaraldehyde

quenching using 10 mg/ml sodium borohydride. Cells were blocked in a 10mg/ml BSA + 10%

goat serum solution. Immunostaining was carried out using a mouse monoclonal CD3 Ab (SC), a

mouse monoclonal anti-CD4 Ab (SC), a mouse monoclonal CD133 Ab (eBioscience), a rat

monoclonal anti-α4 Ab (mAb299) (Whiting and Lindstrom, 1988), a rabbit polyclonal anti-

CDC42 Ab (SC), a monoclonal mouse anti-active-CDC42 (GTP-CDC42) (NewEast

Biosciences), a rabbit polyclonal anti-Gprin1 Ab (Abcam), a mouse monoclonal anti-β-Tubulin

Ab (Cell Signaling), and rhodamine phalloidin (Cell Signaling). Cells were incubated in anti-rat

Dylight 488, anti-mouse Dylight 549, anti-rabbit Dylight 549, and anti-mouse AlexaFluor 647

secondary Abs (ImmunoJackson-Research) and mounted in 0.212% n-Propyl gallate in 90%

glycerol and 10% PBS solution on glass coverslips. Immunostaining was visualized with a Nikon

Eclipse 80i confocal microscope fitted with a Nikon C1 CCD camera and a Zeiss. Cell images

were captured using an EZ-C1 (Nikon) and AxioVision (Zeiss) software.

For cell counts, viable cells were counted using a Trypan Blue (Thermo Scientific) exclusion assay using a C-Chip hemocytometer (INCYTO) under phase contrast. All cells counts were performed in triplicate and the data averaged for each experiment.

Immunohistochemistry and analysis of spleen

Spleen extraction and histological preparation was preformed as described (Lobato-Pascual et al., 2013). Briefly, adult mice were anesthetized using 5% isofluorane and then perfused using 4% paraformaldehyde, pH 7.2. Spleens were dissected then submerged in the paraformaldehyde solution for 24 hours before being transferred to 30% sucrose. Spleens were embedded in 5% agarose and sectioned in the horizontal plane into 40 μm slices using a vibrating blade microtome (Thermo Scientific).

For immunohistochemistry, spleen slices were permeabilized using 0.5% Triton X-100 and quenched by 50 mM ammonium chloride for 30 min at room temp. Tissue was blocked in 10% goat serum then probed with mAb299, a polyclonal anti-Gprin1 Ab (Abcam), a monoclonal anti-CD4 Ab (SC), and a monoclonal anti-CD16 Ab (SC) overnight at 4°C. Dylight secondary Abs (488 and 549) were used. Intact spleens were mounted onto glass slides using the mounting media described above. White and red pulp regions were distinguished by morphology within the intact spleen tissue and in RBC enrichment using DIC.

Cell counts were conducted on fluorescently labeled sections. For total cell counts, a total of 8 spleen sections were stained with the nucleus label DAPI and then counted blindly by 200 μm^2 area. Spleen cell counts are also normalized to total cells of spleen, which was obtained from hemocytometer analysis, relative to size of counting area (200 μm^2).

Immunoprecipitation and western blot

Membrane protein fractions were obtained after solubilization using a non-denaturing lysis

buffer consisting of 1% Triton X-100, 137 mM NaCl, 2 mM EDTA, and 20 mM Tris HCl (pH 8)

with protease (Complete) and phosphatase (Sigma) inhibitor cocktails. This method has been

previously found to enable sufficient solubilization of the nAChR from cells and tissue for

molecular analysis (Nordman and Kabbani, 2012). For the detection of protein-protein

interaction, immunoprecipitation (IP) using the Protein G matrix (Invitrogen) was performed

(Nordman and Kabbani, 2012). Briefly, the IP Ab was bound to a pre-cleared Protein G

Dynabead resin as per manufacturer instructions (Invitrogen). Pure IgG was used to control for

non-specific Ig interaction with the Protein G resin. IP experiments were performed from ICF

preparations at a concentration of 100 μg/ml ICF proteins for Western blot analysis and 750

μg/ml ICF for mass spectrometry analysis. Experiments were performed in triplicates to ensure a

robust result. The primary Abs used for IP and/or Western blotting are: mAb299; polyclonal α4

nAChR (SC; A-20); polyclonal β2 nAChR (SC; H-92); Gα$_o$ (SC); Gprin1 (Abcam); CDC42

(SC); GTP-CDC42 (NewEast Biosciences); NFκB (SC), CD4 (SC); CD16 (SC).

Cell culture

CD3+CD4+ CEMss cells were obtained from Dr. Yuntao Wu (George Mason University). Cells

were grown in RPMI containing 10% fetal bovine serum (FBS) and 1% penicillin-streptomycin

(Pen-strep) antibiotic as per published protocols (Yoder et al., 2008). For transfections, Human

α4 in pcDNA3.1 (provided by Dr. Jerry Stitzel (University of Colorado)), Gprin1 in pcDNA3.1

and Gprin1 siRNA in pRNAT H1.1 (provided by Dr. Law (University of Minnesota)) and

CDC42 in pEGFP/pcDNA3 (provided by Dr. James Bramburg (Colorado State University)) were

transfected using Lipofectamine 2000 as described by the manufacturer (Invitrogen). Cells were transfected with 1 µg/cm^2 cDNA for α4, GFP-Gprin1, GFP-CDC42, and pcDNA3-CDC42. Knockdown of Gprin1 was achieved by transfection with 200 pmol/cm^2 of the Gprin1 siRNA in pRNAT H1.1. An empty pEGFP-C1 or pcDNA vector (Addgene) was used as a transfection control.

ELISA analysis of cytokine levels in plasma and cultured cells

An analysis of cytokines was performed in both plasma fraction of circulating blood of mice or supernatant from cultured cells. For the collection of blood plasma, we used the Ficoll-Paque separation method as described above. For the collection and analysis of cytokines in cultured cells, CEMss cells were treated with nicotine or nicotine and DHβE (for 0, 10, 30, 60, and 120 min) and then centrifuged at slow speed (300 x *g*) for 5 min for supernatant collection. Cytokines were recovered using the Ultracel-3 membrane 3 kDa unit (Amicon). Detection and quantification of IL-6 was conducted using the Rat-Bio ELISA Kit Rat IL-6 (R&D). Detection and quantification of Th1/Th2 cytokines was performed using the Th1/Th2 ELISA Ready-SET-Go! Kit (eBioscience) per manufacturer's instruction.

Mass spectrometry

Liquid chromotagraphy-electro spray ionization (LC-ESI) mass spectrometry (MS) analysis was conducted as described (Nordman and Kabbani, 2012). Select bands were manually excised from coomassie-stained acrylamide gels and then eluted from the gel matrix by alkylation with iodoacetamide and then extracted using trypsin in ammonium bicarbonate. Samples were purified using ZipTips (Millipore) prior to MS analysis using an LTQ-Orbitrap (Thermo).

11

Tandem mass spectra collected by Xcalibur (version2.0.2) were searched against the NCBI rat

protein database using SEQUEST (Bioworks software from ThermoFisher, version 3.3.1). The

SEQUEST search results were filtered using the following criteria: minimum X correlation (XC)

of 1.9, 2.2, and 3.5 for 1+, 2+, and 3+ ions, respectively, and $\Delta Cn > 0.1$. The *Protein Score* (PS)

represents the XC where scores <0.1 were excluded from the analysis. It does not directly reflect

the quantity of the protein or peptides in the sample.

Statistical analysis

Statistical values were obtained using a Student's *t* test or one-way ANOVA. Asterisks indicate

statistical significance in a Student's *t* test, two tailed *P* value, *<0.05; **<0.01; ***<0.001.

Error bars indicate standard error of the mean (SEM). All experiments were performed in

triplicate and group averages are presented.

RESULTS

Detection of α4 nAChR protein expression in immune cells

nAChRs have been identified in immune cells where they play an important role in cholinergic control of immunity (Kawashima and Fujii, 2003; Skok et al., 2007). To determine the expression of α4 nAChRs, we isolated α4-expressing cells (α4+) from blood immune cell fractions (ICF) of mice. The ICF is composed primarily of lymphocytes (~30%) and neutrophils (~50%) (Dhabhar et al., 1995). We developed an immunobead cell-sorting assay (*bead assay*) (Zhichao et al., 2000) to isolate α4+ cells from ICF (Supplementary Fig. 1). The optimization of the bead assay for the detection of cell surface α4 subunits was performed in HEK293 cells that express α4β2 receptors (described in Supplementary Fig. 1) (Sallette et al., 2005). Treatment of these cells with papain was found to be negligible on cell number and nAChR expression (Supplementary Fig. 2). Expression of α4 subunits was confirmed in the α4+ fraction using western blot (Fig. 1A). Knockout mice lacking the α4 subunit (α4-/-) were used as a control for the monoclonal anti-α4 Ab in the assay. A re-probe of the same blot using an anti-β2 Ab shows expression of β2 within the α4+ fraction, consistent with the existence of α4β2 nAChRs in immune cells (Kawashima and Fujii, 2003).

α4+ cells were also analyzed using LC-ESI MS (Supplementary Fig. 1). A cluster of differentiation (CD) system was used for immunophenotyping the α4+ cell fraction. A list of CD markers within the α4+ fraction is presented in Supplementary Table 1. A significant number of T-cell, B-cell, and macrophage cell markers were identified within the α4+ fraction consistent with previous findings on α4 nAChR expression in various immune cells (Kawashima and Fujii, 2003). In particular, a significant number of T-lymphocyte markers were observed in the α4+ fraction including the helper T-cell marker glycoproteins CD4, CD28, CCR4, and CXCR3.

Expression of CD4 was confirmed in α4+ cells derived from the bead assay using immunoblotting (Fig. 1A). Our findings verify that a portion of α4+ cells also express CD4 (α4+CD4+) but CD4 can also be expressed on macrophages and dendritic cells, therefore we probed the α4+ fraction with a CD16 Ab to assess the level of macrophage, neutrophil, and NK cells. As shown in Fig. 1A, CD16 expression was lower than CD4 expression in the α4+ fraction suggesting that the majority of α4 receptors are on T-cells.

Fluorescence activated cell sorting (FACS) and immunocytochemistry were used to further characterize α4+ cells in ICF. Similar to previous studies (Darsow et al., 2005), α4+ cells were isolated by FACS and found to constitute 3.9% of the total ICF (Fig. 1B). FACS experiments from α4-/- mice show a <0.1% detection of the Ab signal (Supplementary Fig. 2C). FACS was also used to analyze α4+ cells isolated from the ICF using the bead assay (Supplementary Fig. 1). CD4+ cells accounted for 23.0% of the α4+ population (Fig. 1C) consistent with earlier findings on CD4 expression (Fig. 1A). Cell suspensions of ICF were stained with anti α4 nAChR, CD3, and CD4 Abs. As shown in Fig. 1D and Supplementary Fig. 2D, immunolabeling shows a noticeable portion of the ICF population cells expressing α4, CD4, and CD3 proteins. Moreover, ~7.8% of CD3+ ICF population were found to co-express α4 and CD4 proteins, confirming the existence of an α4 nAChR T-cell population in blood. ICF from α4-/- did not show strong immunoreactivity to the α4 Ab in the analysis (Fig. 1D) supporting the specificity of the mAb299 in the experiment.

Characterization of an α4 nAChR signaling apparatus in immune cells

Receptors are components of large protein complexes (interactomes) underlying the mechanisms of receptor signaling and regulation in cells (Kabbani et al., 2007). To explore interactions of the

α4 nAChR, we coupled co-immunoprecipitation and LC-ESI MS (Nordman and Kabbani, 2012) to define α4 nAChR interacting proteins in immune cells (Supplementary Fig. 1). In these experiments, ICF from α4-/- mice were used as a negative control for the immunoprecipitating anti-α4 nAChR Ab (mAb299). As shown in Fig. 1E, an interaction network comprising G protein regulated-inducer of neurite outgrowth 1 (Gprin1), Gα$_o$, the β2 nAChR subunit, and cell division control protein 42 (CDC42) was detected within the immunoprecipitated α4 nAChR fraction from ICF. The shown gel illustrates the position of protein bands co-immunoprecipitated with the α4 nAChR. The identity of the proteins was confirmed using MS peptide analysis (Supplementary Table 2) and western blotting (Fig. 1E). Gprin1 and Gα$_o$ have been shown to bind nAChRs in neural cells (Nordman and Kabbani, 2012) suggesting that the interactions are common to neural and immune cells.

Gprin1 is found to regulate the signaling and localization of opioid and nAChRs (Ge et al., 2009; Nordman and Kabbani, 2012). We validated interactions between α4 nAChRs and Gprin1 in immune cells by immunoprecipitating Gprin1 from the ICF and identifying the components of its interactome using the same proteomic approach. IgG was used as a negative control for immunoprecipitation. Gprin1 Abs have been used by us for immunoprecipitation studies (Nordman and Kabbani, 2012). As shown in Fig. 1E, Gprin1 and α4 nAChRs share common binding partners in immune cells. Coexpression of α4 and Gprin1 was verified in CD4+ cells using an anti-CD4 bead assay. An immunostaining of these cells with α4 and Gprin1 Abs demonstrates coexpression of the proteins in immune cells and their colocalization at f-actin rich membrane domains (Fig. 1F).

α4 nAChRs regulate CD4+ T-cell proliferation

CD4+ cells play an important role in immune function by supporting the activity of B-cells and macrophages (Itano and Jenkins, 2003). We assayed expression and interaction of α4 nAChRs within ICF from circulating blood (ICF_C), spleen (ICF_S), and thymus (ICF_T). As shown in Fig. 2A, immunoreactivity for α4 nAChRs, CD4, and Gprin1 was detected in all 3 fractions ($ICF_{C/S/T}$). GAPDH was used as a loading control. Studies indicate an effect of chronic nicotine on cytokine and Ab production (Skok et al., 2007; Song et al., 1999). We examined the effects of a 6-day (sustained) nicotine treatment (0.5-1.0 mg/kg) in mice. Nicotine injections were also performed in α4-/- mice. A dose dependent increase in spleen and thymus weight was observed in response to nicotine treatment in WT mice (Fig. 2B and Figs. S3-S4). Nicotine did not dramatically alter the size of the spleen or thymus in α4-/- mice, suggesting that α4 expression is necessary for the effect.

Next we quantified cells in the $ICF_{C/S/T}$. Consistent with its effect on organ size, nicotine was found to increase cell number in a dose dependent manner at the tested doses of 0.1-1.5 mg/kg body weight in the $ICF_{C/S/T}$ of mice (Fig. 2C, Supplementary Fig. 3B and 4B). We did not detect a change in cell number in α4-/- mice in response to nicotine (Fig. 2C). To examine cell specific effects of nicotine, we analyzed the ICF_S by FACS. Nicotine was found to increase α4+ cells by 4.8%; α4+CD4+ cells by 7.1%; CD4+ cells by 5.1%; and CD3+CD4+ cells by 1.9% (Fig. 2D). A similar analysis of ICF_S from α4-/- mice exposed to nicotine showed a negligible rise in CD4+ cells (0.4%) and CD3+CD4+ cells (0.4%) (Fig. 2D) suggesting that α4 nAChRs contribute to nicotine mediated T-cell proliferation.

16

α4 and Gprin1 expressing helper T-cells respond to nicotine

Studies show that nAChRs play a role in immune function in the spleen (Tracey, 2009). We have determined an expression of α4 nAChRs in immune cells of spleen, thymus, and circulation (Fig. 2A). Next we immunohistochemically examined the distribution of α4 nAChRs and Gprin1 in the spleen. Cells were also labeled with the T-helper cell marker CD4 or the macrophage, neutrophil, and NK marker CD16. The spleen is divided into two main compartments: white pulp, which is abundant in T- and B- lymphocytes, and red pulp, which is abundant in RBCs and macrophages (Barnhart and Lusher, 1976). As shown in Fig 3A, Gprin1 immunolableing was seen in both red and white pulp regions. α4+CD4+ expression on the other hand appeared localized to the white pulp (Fig. 3A) consistent with the role of α4 nAChRs in T-cell function. A quantitative assessment of the immunolabeling indicates that the majority of α4+CD4+ cells also express Gprin1 (Fig. 3A and 3C) and CD3 (data not shown). A subset of CD16+ cells was also found to stain for Gprin1 (data not shown).

Human smoking is associated with spleen disorders such as extramedullary hemaptopoiesis (Pandit et al., 2006) and splenomegaly (Kupfer, 1992). We explored the effect of nicotine on T-cell proliferation in the spleen. As indicated in Figs. 3B and 3C, nicotine was found to augment the percentage of α4+ (+4.4%) and CD4+ (+2.4%) cells in the white pulp relative to total cell counts per the same 200 μm^2 area. Nicotine was also found to increase the ratio of α4+CD4+Gprin1+ cells in the spleen (+1.9%) (Fig. 3C). This finding was confirmed in a staining of the ICF$_S$ which showed a 3% rise in the α4+CD4+Gprin1+ cell population (Fig. 3D) in response to nicotine. Experiments in α4-/- mice show that nicotine only marginally increases CD4+ cell number (+1.1% (data not shown)) underscoring the role of α4 nAChRs in the process.

T-cell proliferation is associated with changes in cytoskeletal signaling (Muller et al., 2006). We explored the effect of nicotine on the localization of α4 nAChRs and Gprin1 in CD4+ cells from the ICF$_S$ of nicotine treated mice. The specificity of the anti- α4 Ab (mAb299) was tested in α4-/- mice (Fig. 1D-E; Fig. 3B). The specificity of the anti-Gprin1 Ab in immunocytochemical analysis was tested in cultured T-cells that showed a correlation between the Ab signal and Gprin1 expression in the cell (Supplementary Fig. 5). As shown in Fig. 3E, nicotine was found to alter the distribution of α4 nAChRs and Gprin1 in CD4+ cells. In particular, nicotine promoted a translocation of Gprin1 from the cytosol to the plasma membrane in dividing cells (Fig. 3E). In CD4+ cells of α4-/- mice, nicotine did not alter Gprin1 expression.

Nicotine promotes proliferation of α4+/Gprin1+/CD4+ cells in the bone marrow

To determine the effect of nicotine on T-cell proliferation in the bone marrow, mice were injected with nicotine (0.5 and 1.0 mg/kg) for 6 days. Consistent with its effects in the ICF$_{C/S/T}$, nicotine also increased the total number of cells in the bone marrow fraction (BMF) (Fig. 4A). Since smoking has been shown to influence hematopoiesis (Chang et al., 2010; Pandit et al., 2006), the BMF was immunolabeled for α4, Gprin1, CD4, and the hematopoietic stem cell marker CD133 (Yin et al., 1997). As shown in Fig. 4B-C, α4+ cells in the BMF were found to express CD4+ or CD133+ proteins. Most α4+ cells were also immunoreactive for the anti-Gprin1 Ab (Fig. 4B-C), which was detected throughout the BMF (data not shown). Treatment with nicotine was found to increase the number of α4+Gprin1+ cells in the BMF but this effect was not found to be statistically significant (saline: 25% of total (±4%); 0.5 mg/kg nicotine: 27% of total (± 4%), p=0.54; 1.0 mg/kg nicotine: 31% (±3%), p=0.23). Consistent with findings in the spleen (Fig. 3C), nicotine was found to significantly enhance the number of α4+Gprin1+CD4+

cells and in a dose-dependent manner (Fig. 4C-D). In contrast, nicotine treatment was found to decrease the overall number of α4+Gprin1+CD133+ cells in the BMF, suggesting that nicotine may promote stem cell proliferation.

α4 nAChRs signal via CDC42 in T-cells

While nAChRs are known to play an important role in immune function (Tracey, 2009), little is known about their intracellular signaling in immune cells. We utilized a human T4-lymphoblastoid cell line, CEMss (CD3+CD4+) to elucidate α4 nAChR signaling in T-cells (Yoder et al., 2008). This T-cell line also endogenously expresses α4 and β2 nAChRs as well as Gprin1 (Fig. 5A), enabling the study of this pathway endogenously. An IP of the α4 nAChR validated interaction between the α4β2 nAChR and Gprin1 (Fig. 5A). Nicotine and ACh are mitogenic agents in some immune cells (Hawkins et al., 2002). Similar to our observations on CD4+ cells *in vivo* (Fig. 2), we found that nicotine significantly promotes proliferation of CEMss cells. As shown in Fig. 5B, nicotine treatment was associated with a dose dependent increase in T-cell number which was abolished by the α4β2 nAChR specific-antagonist dihydro-β-erythroidine (DHβE).

CDC42, a rho GTPase, can mediate actin polymerization leading to changes in cytokine release and T-cell division (Guo et al., 2010). $G\alpha_o$ and Gprin1 have been shown to regulate CDC42 activity in neural cells (Nakata and Kozasa, 2005) while $G\alpha_o$ is found to also regulate CDC42 in T-cells (Garcia-Bernal et al., 2011). Based on the discovery of an interaction between α4 nAChRs, Gprin1, $G\alpha_o$, and CDC42 (Fig. 1E), we hypothesize that α4 nAChRs operate via a Gprin1 pathway to regulate CDC42 in T-cells. To test this, CEMss cells were transiently transfected with Gprin1 (pcDNA3.1), Gprin1 RNAi (pRNAT H1.1), or CDC42 (pEGFP)

19

expression vectors. Preliminary studies show that transfection of these cells with constructs encoding Gprin1 and CDC42 increases their respective protein levels by 108% and 94%. Transfection with Gprin1 siRNA reduces Gprin1 protein expression by 87% (Supplementary Fig. 5). As shown in Fig. 5C, nicotine had little or no effect on T-cell proliferation in cells overexpressing Gprin1 or CDC42. In contrast, T-cell proliferation was significantly enhanced following transfection with Gprin1 siRNA and nicotine treatment. Indeed even in the absence of nicotine, Gprin1 siRNA was found to increase T-cell number by 52% (data not shown). Involvement of $G\alpha_o$ was established by examining the effects of the $G\alpha_o$ activator mastopran (MSP) on nicotine treatment (Yamauchi et al., 2000). As shown in Fig. 5C, nicotine did not effect T-cell proliferation in the presence of MSP, confirming a role for $G\alpha_o$ in the pathway. These results suggest that Gprin1 inhibits (nicotine-mediated) T-cell proliferation, possibly via the negative regulation of CDC42.

T-cell proliferation and cytokine release are mediated by GTP activation of CDC42 (Su et al., 2005). Using an Ab selective for CDC42 in the GTP bound state (GTP-CDC42) we determined the effect of nicotine on CDC42. CDC42 was found in T-cells and appeared to colocalize with Gprin1 in actin rich domains (Fig. 5D). We found a dose-dependent reduction in GTP-CDC42 expression following nicotine treatment (Fig. 5E), and detected an effect at levels below its EC50, suggesting that low levels achieved by smokers (<1uM) (Russell et al., 1980) contribute to immunity. The effect of nicotine was abolished by DHβE confirming the role of α4β2 nAChRs in CDC42 activation. A similar effect of nicotine on CDC42 was observed in vivo. GTP-CDC42 expression was significantly reduced in ICF$_s$ of mice treated with nicotine while a small increase in GTP-CDC42 levels was observed in nicotine treated α4-/- mice (Fig. 5F). Total CDC42 levels appeared unaltered (data not shown).

The involvement of Gprin1 in the activation of CDC42 was also tested. As shown in Fig. 5G, a knockdown of Gprin1 protein expression (via siRNA) was found to decrease CDC42 activation (-90% GTP-CDC42 levels) in the cell. In T-cells with reduced Gprin1, nicotine did not affect GTP-CDC42 levels suggesting that Gprin1 is necessary for nicotine mediated CDC42 regulation. This is consistent with results showing that the overexpression of CDC42 in the cell is sufficient to override the effects of Gprin1 siRNA on GTP-CDC42 levels (Fig. 5G) and indicate that CDC42 is regulated downstream of Gprin1 in the pathway. Taken together, the data presents a new mechanism of α4 nAChR signaling in T-cells involving Gprin1 modulation of CDC42.

Nicotine promotes Th2 immunity via the α4 nAChR

Helper T-cells play an important role in mediating the immune response via the distinct actions of Th1 and Th2 cell types (Cocks et al., 1995). A change in the Th1/Th2 ratio has been examined via detection of cell surface markers such as the chemokine receptors CXCR3 and CCR4 as well as the release of specific cytokines (Cocks et al., 1995). Nicotine has previously been found to promote a Th2 immune response in CD4 T-cells (Zhang and Petro, 1996). We examined the role of α4 nAChRs in the nicotine-associated immune response of T-cells. As shown in Fig. 6, a significant increase in the level of Th2 cytokines (IL-4, IL-6 and IL-10) was detected in mice treated with nicotine for 6 days. In comparison, nicotine had little effect on Th1 cytokine (IFN-γ or IL-2) levels (Fig. 6). Because cytokine levels did not change in α4-/- mice following sustained nicotine treatment, we presume the α4 nAChR to be necessary for these Th2 responses.

We assessed cytokine release in cultured T-cells. CEMss cells were treated with nicotine (0-120 min) and then analyzed for IFN-γ, IL-2, IL-4, IL-6 and IL-10 release. As shown in Fig. 6,

nicotine treatment significantly increased Th2 cytokine release from T-cells but failed to do so in the presence of DHβE (which was also found to decrease IL-4 release from the cell). We also found that nicotine attenuated the levels of the Th1 cytokine IFN-γ released from T-cells and this effect was also abolished by DHβE (Fig. 6). IL-2 release however appeared unaffected by nicotine treatment suggesting that α4 nAChRs regulate the release of Th2 cytokines from T-cells.

An α4 nAChR signaling mechanism for IL-6 release from T-cells

IL-6 has been shown to promote a Th2 response via activation of immature helper T-cells (Diehl and Rincon, 2002). We hypothesize that α4 nAChRs regulate IL-6 release via the Gprin1/CDC42 pathway. To test this, we examined the effects of Gprin1 and CDC42 overexpression as well as Gprin1 knockdown on IL-6 release after nicotine treatment. As shown in Fig. 7A, nicotine was found to increase IL-6 release from T-cells consistent with earlier reports (Kondo et al., 2010) and our observations *in vivo* (Fig. 6). In response to nicotine, cells transfected with cDNA for Gprin1 or CDC42 did not present an increase in IL-6 release compared to controls, while cells transfected with Gprin1 siRNA appeared to release more IL-6 suggesting that Gprin1 inhibits cytokine production/release in the presence of nicotine.

To determine if the synthesis of IL-6 was affected, immunoblot analysis of total IL-6 expression in T-cells was performed. As shown in Fig. 7B, IL-6 production increased in response to nicotine consistent with data on IL-6 release. In cells transfected with Gprin1 siRNA, IL-6 levels also increased revealing an effect of Gprin1 on cytokine production as well as release. Transfection of cells with Gprin1 or CDC42 cDNA as well as treatment with nicotine in the presence of DHβE appeared to decrease IL-6 production (Fig. 7B) as it did for release. These results demonstrate that IL-6 production and release are coupled in T-cells and that α4 nAChR

signaling via Gprin1 and CDC42 regulates cytokine production and release. In particular, Gprin1 and CDC42 appear to block the production and release of IL-6 from T-cells.

We imaged CEMss cells for IL-6 expression in the presence and absence of nicotine. As expected, nicotine was found to augment the expression of IL-6 (+31.1%) in T-cells (Fig. 7C-D). Specifically nicotine was found to enhance IL-6 expression in vesicle-like structures, and promote its localization at tubulin and actin rich regions of the plasma membrane (Fig. 7C), suggestive of enhanced released. Nicotine mediated IL-6 expression was diminished by the addition of DHβE resulting in a decrease in the immunofluorescence and western blot signal of IL-6 in T-cells (Fig. 7B-D). Cell image data strongly corroborates biochemical findings in these studies highlighting a role for α4 nAChR in IL-6 localization and possible release. Lastly, involvement of Gprin1 in α4 nAChR signaling was established by the findings that Gprin1 overexpression diminishes the number of IL-6 expressing cells (-9.5%) and IL-6 fluorescence within vesicle like structures (-14.8%), even in the presence of nicotine (Fig. 7C-D).

DISCUSSION

The immune system functions to modulate inflammation and stress response throughout the body (Rius et al., 2008). The contributions of nAChRs to immunity have emerged well after the discovery of nAChR expression in immune cells over 30 years ago (Lennon, 1976). In this study we show that nicotine promotes CD4+ T-cell function via the α4 nAChR. Although cigarette smoke contains more than just nicotine, the observed effects of nicotine in this study advocate an important role for this substance on T-cell driven immunity (Sopori, 2002). α4 nAChRs may thus play a central role in the actions of nicotine on T-cells and inflammation leading to an increased susceptibility to immune diseases such as Crohn's disease and rheumatoid arthritis (Sopori, 2002). Interestingly, these same receptors may also contribute to the protective effects of nicotine in conditions such as ulcerative colitis and Parkinson's disease (Guslandi, 1999; Quik et al., 2012).

Nicotine promotes Th2 immunity via the α4 nAChR

The lack of electrophysiological data on nAChR function in immune cells has stymied explanations on their contributions to immunity. Signaling through α7 nAChRs has been found to attenuate the production of cytokines, such as TNF-α, in monocytes and macrophages contributing to the parasympathetic response of the hypothalamic pituitary axis (Rosas-Ballina et al., 2011). This response can activate a subset of ACh producing T-cells within the white pulp region of the spleen (Rosas-Ballina et al., 2011), an area we find to be strong in α4 and Gprin1 protein expression. By operating through a Gprin1/CDC42 signaling pathway, α4 nAChRs are implicated in T-cell proliferation and cytokine production. In the bone marrow, nicotine is found to alter stem cell number, suggestive of a role for nicotine in hematopoiesis within α4 expressing

cells. Whether the opening of the nAChR channel is necessary for the actions of nicotine in the immune system is still enigmatic. Our experiments suggest that at minimum nicotine can foster an enhanced nAChR response via the pharmacological chaperoning of the receptor in T-cells and the activation of the Gprin1/CDC42 pathway resulting in cell proliferation and IL-6 release. Because the effects of nicotine on T-cell proliferation and cytokine release were not detected in α4-/- mice, our findings underscore the role for the α4 subunit in the immune response but cannot dismiss the contributions of other nAChRs including β2.

In one scenario, it is possible that IL-6 release is intimately associated with the release of additional Th2 cytokines from T-cells, shifting the immune response into Th2 immunity (Diehl and Rincon, 2002). Studies have shown that IL-4 production promotes IL-6 release via a similar Rac/CDC42 pathway in keratinocytes (Wery-Zennaro et al., 2000), consistent with our observations on the release time course of the two cytokines in T-cells. Th2 immunological responses are associated with adaptive immunity and increases in IgE antibody production (Ujike et al., 2002). If nicotine is indeed found to trigger Th2 immunity in humans, our study may begin to explain the molecular connection between cigarette smoke and autoimmune disease as supported by epidemiological evidence (Costenbader et al., 2006). For example, since both nicotine smoke and enhanced IL-6 production are shown to increase the symptoms of autoimmune diseases such as myasthenia gravis (MG) and Crohn's disease (Aricha et al., 2011; Maniaol et al., 2013), it is interesting to consider that nicotine can directly promote IL-6 production in T-cells via the α4 nAChR.

Interaction with Gprin1 mediates α4 nAChR signaling in T cells

Cytokines released from T-lymphocytes undergo at least four regulatory checkpoints: differentiation, transcription, translation, and secretion (Cohen et al., 1974). In particular, cytokines secreted by activated CD4+ T-cells appear to exit the cell via remodeling of the cytoskeleton (Yoder et al., 2008). Our experiments in cultured T-cells likely only address the later points. As shown in Fig. 8, our data demonstrates that nicotine, operating through an α4 nAChR/Gprin1/CDC42 pathway, can promote the formation of budding cytokine-containing vesicles via actions on the cytoskeleton, suggestive of cytokine release. This process appears dependent on the function of the α4 nAChR and the $G\alpha_o$ and Gprin1 protein complex, which can regulate the activity of CDC42. A similar $G\alpha_o$/Gprin1 mechanism of CDC42 regulation exists in neural cells and regulates neurite formation (Nakata and Kozasa, 2005; Nordman et al., 2013). Inhibition of CDC42 in T-cells is found to regulate the polymerization of actin to f-actin (Yoder et al., 2008), leading to changes in (IL-6) cytokine vesicle loading and release. This is in agreement with earlier finding that CDC42 regulates the concentration and secretion of vesicles containing a similar cytokine (IFN-γ) in T-cells (Chemin et al., 2012).

In addition, CDC42 may also contribute to cytokine production via NFκB (Hobert et al., 2002). Recent studies show that NFκB is regulated by β2 containing nAChRs in immune cells (Hao et al., 2013). Based on our findings of an interaction between NFκB and the α4 nAChR interactome (Fig. 1E), it is plausible that NFκB also operates in the nicotine driven α4 nAChR pathway underlying T-cell function.

ACKNOWLEDGMENTS

AUTHORSHIP CONTRIBUTIONS

Participated in research design: Nordman and Kabbani.

Conducted experiments: Nordman, Muldoon, and Clark.

Contributed new reagents or analytic tools: Kabbani and Damaj.

Performed data analysis: Nordman.

Wrote or contributed to the writing of the manuscript: Nordman and Kabbani.

REFERENCES

Amin RH, Chen HQ, Veluthakal R, Silver RB, Li J, Li G and Kowluru A (2003) Mastoparan-induced insulin secretion from insulin-secreting betaTC3 and INS-1 cells: evidence for its regulation by Rho subfamily of G proteins. *Endocrinology* **144**(10): 4508-4518.

Andersson J (2005) The inflammatory reflex--introduction. *Journal of internal medicine* **257**(2): 122-125.

Aricha R, Mizrachi K, Fuchs S and Souroujon MC (2011) Blocking of IL-6 suppresses experimental autoimmune myasthenia gravis. *J Autoimmun* **36**(2): 135-141.

Barnhart MI and Lusher JM (1976) The human spleen as revealed by scanning electron microscopy. *American journal of hematology* **1**(2): 243-264.

Chang E, Forsberg EC, Wu J, Bingyin W, Prohaska SS, Allsopp R, Weissman IL and Cooke JP (2010) Cholinergic activation of hematopoietic stem cells: role in tobacco-related disease? *Vasc Med* **15**(5): 375-385.

Changeux JP (2010) Nicotine addiction and nicotinic receptors: lessons from genetically modified mice. *Nature reviews Neuroscience* **11**(6): 389-401.

Chemin K, Bohineust A, Dogniaux S, Tourret M, Guegan S, Miro F and Hivroz C (2012) Cytokine secretion by CD4+ T cells at the immunological synapse requires Cdc42-dependent local actin remodeling but not microtubule organizing center polarity. *J Immunol* **189**(5): 2159-2168.

Cocks BG, Chang CC, Carballido JM, Yssel H, de Vries JE and Aversa G (1995) A novel receptor involved in T-cell activation. *Nature* **376**(6537): 260-263.

Cohen S, Bigazzi PE and Yoshida T (1974) Commentary. Similarities of T cell function in cell-mediated immunity and antibody production. *Cell Immunol* **12**(1): 150-159.

Cormier A, Paas Y, Zini R, Tillement JP, Lagrue G, Changeux JP and Grailhe R (2004) Long-term exposure to nicotine modulates the level and activity of acetylcholine receptors in white blood cells of smokers and model mice. *Molecular pharmacology* **66**(6): 1712-1718.

Costenbader KH, Feskanich D, Mandl LA and Karlson EW (2006) Smoking intensity, duration, and cessation, and the risk of rheumatoid arthritis in women. *Am J Med* **119**(6): 503 e501-509.

Costenbader KH and Karlson EW (2005) Cigarette smoking and systemic lupus erythematosus: a smoking gun? *Autoimmunity* **38**(7): 541-547.

Darsow T, Booker TK, Pina-Crespo JC and Heinemann SF (2005) Exocytic trafficking is required for nicotine-induced up-regulation of alpha 4 beta 2 nicotinic acetylcholine receptors. *J Biol Chem* **280**(18): 18311-18320.

Davis R, Rizwani W, Banerjee S, Kovacs M, Haura E, Coppola D and Chellappan S (2009) Nicotine promotes tumor growth and metastasis in mouse models of lung cancer. *PLoS One* **4**(10): e7524.

Dhabhar FS, Miller AH, McEwen BS and Spencer RL (1995) Effects of stress on immune cell distribution. Dynamics and hormonal mechanisms. *J Immunol* **154**(10): 5511-5527.

Diehl S and Rincon M (2002) The two faces of IL-6 on Th1/Th2 differentiation. *Molecular immunology* **39**(9): 531-536.

Garcia-Bernal D, Dios-Esponera A, Sotillo-Mallo E, Garcia-Verdugo R, Arellano-Sanchez N and Teixido J (2011) RGS10 restricts upregulation by chemokines of T cell adhesion mediated by alpha4beta1 and alphaLbeta2 integrins. *J Immunol* **187**(3): 1264-1272.

Ge X, Qiu Y, Loh HH and Law PY (2009) GRIN1 regulates micro-opioid receptor activities by tethering the receptor and G protein in the lipid raft. *J Biol Chem* **284**(52): 36521-36534.

Guo F, Hildeman D, Tripathi P, Velu CS, Grimes HL and Zheng Y (2010) Coordination of IL-7 receptor and T-cell receptor signaling by cell-division cycle 42 in T-cell homeostasis. *Proc Natl Acad Sci U S A* **107**(43): 18505-18510.

Guslandi M (1999) Nicotine treatment for ulcerative colitis. *Br J Clin Pharmacol* **48**(4): 481-484.

Hao J, Shi FD, Abdelwahab M, Shi SX, Simard A, Whiteaker P, Lukas R and Zhou Q (2013) Nicotinic Receptor beta2 Determines NK Cell-Dependent Metastasis in a Murine Model of Metastatic Lung Cancer. *PLoS One* **8**(2): e57495.

Hawkins BT, Brown RC and Davis TP (2002) Smoking and ischemic stroke: a role for nicotine? *Trends Pharmacol Sci* **23**(2): 78-82.

Hobert ME, Sands KA, Mrsny RJ and Madara JL (2002) Cdc42 and Rac1 regulate late events in Salmonella typhimurium-induced interleukin-8 secretion from polarized epithelial cells. *J Biol Chem* **277**(52): 51025-51032.

Hoff J (2000) Methods of Blood Collection in the Mouse. *Lab Animal* **29**(10): 47-53.

Itano AA and Jenkins MK (2003) Antigen presentation to naive CD4 T cells in the lymph node. *Nat Immunol* **4**(8): 733-739.

Kabbani N, Woll MP, Levenson R, Lindstrom JM and Changeux JP (2007) Intracellular complexes of the beta2 subunit of the nicotinic acetylcholine receptor in brain identified by proteomics. *Proceedings of the National Academy of Sciences of the United States of America* **104**(51): 20570-20575.

Kawashima K and Fujii T (2003) The lymphocytic cholinergic system and its contribution to the regulation of immune activity. *Life sciences* **74**(6): 675-696.

Kondo Y, Tachikawa E, Ohtake S, Kudo K, Mizuma K, Kashimoto T, Irie Y and Taira E (2010) Inflammatory cytokines decrease the expression of nicotinic acetylcholine receptor during the cell maturation. *Mol Cell Biochem* **333**(1-2): 57-64.

Kupfer S (1992) [A case from practice (248). 1. Chronic idiopathic thrombocytopenic purpura with discrete splenomegaly. 2. Chronic HBV infection. Incomplete vital antigen synthesis. Minimal inflammation without signs of aggression. 3. Subacute cytomegalovirus infection (laboratory diagnosis). 4. Status following hepatitis A. 5. Nicotine abuse]. *Schweiz Rundsch Med Prax* **81**(33): 968-970.

Lennon VA (1976) Immunology of the acetylcholine receptor. *Immunol Commun* **5**(4): 323-344.

Lobato-Pascual A, Saether PC, Dahle MK, Gaustad P, Dissen E, Fossum S and Daws MR (2013) Rat macrophage C-type lectin is an activating receptor expressed by phagocytic cells. *PLoS One* **8**(2): e57406.

Maniaol AH, Boldingh M, Brunborg C, Harbo HF and Tallaksen CM (2013) Smoking and socio-economic status may affect myasthenia gravis. *Eur J Neurol* **20**(3): 453-460.

Marubio LM, del Mar Arroyo-Jimenez M, Cordero-Erausquin M, Lena C, Le Novere N, de Kerchove d'Exaerde A, Huchet M, Damaj MI and Changeux JP (1999) Reduced antinociception in mice lacking neuronal nicotinic receptor subunits. *Nature* **398**(6730): 805-810.

Marubio LM, Gardier AM, Durier S, David D, Klink R, Arroyo-Jimenez MM, McIntosh JM, Rossi F, Champtiaux N, Zoli M and Changeux JP (2003) Effects of nicotine in the dopaminergic system of mice lacking the alpha4 subunit of neuronal nicotinic acetylcholine receptors. *The European journal of neuroscience* **17**(7): 1329-1337.

Middlebrook AJ, Martina C, Chang Y, Lukas RJ and DeLuca D (2002) Effects of nicotine exposure on T cell development in fetal thymus organ culture: arrest of T cell maturation. *Journal of immunology* **169**(6): 2915-2924.

Moreau T, Depierre P, Brudon F and Confavreux C (1994) Nicotine-sensitive myasthenia gravis. *Lancet* **344**(8921): 548-549.

Muller N, Avota E, Schneider-Schaulies J, Harms H, Krohne G and Schneider-Schaulies S (2006) Measles virus contact with T cells impedes cytoskeletal remodeling associated with spreading, polarization, and CD3 clustering. *Traffic* **7**(7): 849-858.

Nakata H and Kozasa T (2005) Functional characterization of Galphao signaling through G protein-regulated inducer of neurite outgrowth 1. *Molecular pharmacology* **67**(3): 695-702.

Nordman JC and Kabbani N (2012) An interaction between alpha7 nicotinic receptors and a G-protein pathway complex regulates neurite growth in neural cells. *Journal of cell science* **125**(Pt 22): 5502-5513.

Nordman JC, Philips WS, Kodama N, Clark SG, Del Negro C and Kabbani N (2013) Axon Targeting and Function of the Alpha 7 Nicotinic Receptor in Developing Hippocampal Neurons via Gprin1. *Journal of Cell Science* **In press**.

Pandit TS, Sikora L, Muralidhar G, Rao SP and Sriramarao P (2006) Sustained exposure to nicotine leads to extramedullary hematopoiesis in the spleen. *Stem Cells* **24**(11): 2373-2381.

Quik M, Perez XA and Bordia T (2012) Nicotine as a potential neuroprotective agent for Parkinson's disease. *Mov Disord* **27**(8): 947-957.

Rius J, Guma M, Schachtrup C, Akassoglou K, Zinkernagel AS, Nizet V, Johnson RS, Haddad GG and Karin M (2008) NF-kappaB links innate immunity to the hypoxic response through transcriptional regulation of HIF-1alpha. *Nature* **453**(7196): 807-811.

Rosas-Ballina M, Olofsson PS, Ochani M, Valdes-Ferrer SI, Levine YA, Reardon C, Tusche MW, Pavlov VA, Andersson U, Chavan S, Mak TW and Tracey KJ (2011) Acetylcholine-synthesizing T cells relay neural signals in a vagus nerve circuit. *Science* **334**(6052): 98-101.

Ross SA, Wong JY, Clifford JJ, Kinsella A, Massalas JS, Horne MK, Scheffer IE, Kola I, Waddington JL, Berkovic SF and Drago J (2000) Phenotypic characterization of an alpha 4 neuronal nicotinic acetylcholine receptor subunit knock-out mouse. *The Journal of neuroscience : the official journal of the Society for Neuroscience* **20**(17): 6431-6441.

Russell MA, Jarvis M, Iyer R and Feyerabend C (1980) Relation of nicotine yield of cigarettes to blood nicotine concentrations in smokers. *Br Med J* **280**(6219): 972-976.

Sallette J, Pons S, Devillers-Thiery A, Soudant M, Prado de Carvalho L, Changeux JP and Corringer PJ (2005) Nicotine upregulates its own receptors through enhanced intracellular maturation. *Neuron* **46**(4): 595-607.

Skok MV, Grailhe R, Agenes F and Changeux JP (2007) The role of nicotinic receptors in B-lymphocyte development and activation. *Life sciences* **80**(24-25): 2334-2336.

Song DK, Im YB, Jung JS, Suh HW, Huh SO, Song JH and Kim YH (1999) Central injection of nicotine increases hepatic and splenic interleukin 6 (IL-6) mRNA expression and plasma IL-6 levels in mice: involvement of the peripheral sympathetic nervous system. *FASEB journal : official publication of the Federation of American Societies for Experimental Biology* **13**(10): 1259-1267.

Sopori M (2002) Effects of cigarette smoke on the immune system. *Nat Rev Immunol* **2**(5): 372-377.

Su IH, Dobenecker MW, Dickinson E, Oser M, Basavaraj A, Marqueron R, Viale A, Reinberg D, Wulfing C and Tarakhovsky A (2005) Polycomb group protein ezh2 controls actin polymerization and cell signaling. *Cell* **121**(3): 425-436.

Tracey KJ (2009) Reflex control of immunity. *Nat Rev Immunol* **9**(6): 418-428.

Ujike A, Takeda K, Nakamura A, Ebihara S, Akiyama K and Takai T (2002) Impaired dendritic cell maturation and increased T(H)2 responses in PIR-B(-/-) mice. *Nat Immunol* **3**(6): 542-548.

Wery-Zennaro S, Zugaza JL, Letourneur M, Bertoglio J and Pierre J (2000) IL-4 regulation of IL-6 production involves Rac/Cdc42- and p38 MAPK-dependent pathways in keratinocytes. *Oncogene* **19**(12): 1596-1604.

Whiting PJ and Lindstrom JM (1988) Characterization of bovine and human neuronal nicotinic acetylcholine receptors using monoclonal antibodies. *The Journal of neuroscience : the official journal of the Society for Neuroscience* **8**(9): 3395-3404.

Yamauchi J, Kawano T, Nagao M, Kaziro Y and Itoh H (2000) G(i)-dependent activation of c-Jun N-terminal kinase in human embryonal kidney 293 cells. *J Biol Chem* **275**(11): 7633-7640.

Yin AH, Miraglia S, Zanjani ED, Almeida-Porada G, Ogawa M, Leary AG, Olweus J, Kearney J and Buck DW (1997) AC133, a novel marker for human hematopoietic stem and progenitor cells. *Blood* **90**(12): 5002-5012.

Yoder A, Yu D, Dong L, Iyer SR, Xu X, Kelly J, Liu J, Wang W, Vorster PJ, Agulto L, Stephany DA, Cooper JN, Marsh JW and Wu Y (2008) HIV envelope-CXCR4 signaling activates cofilin to overcome cortical actin restriction in resting CD4 T cells. *Cell* **134**(5): 782-792.

Zhang S and Petro TM (1996) The effect of nicotine on murine CD4 T cell responses. *Int J Immunopharmacol* **18**(8-9): 467-478.

Zhichao C, Yong Y and Ping Z (2000) Methodological study of cell separation with domestic immunomagnetic beads. *Journal of Tongji Medical University* **20**(3): 208-209.

FOOTNOTES

FIGURE LEGENDS

FIGURE 1. Isolation of α4 nAChRs and their signaling partners in CD4+ cells. (A) Western blot

detection of α4 and β2 nAChRs, CD4, and CD16 within the α4+ fraction isolated from ICF_C

using the bead assay (n=3 mice for WT and α4-/-). IgG beads (+ lane) and ICF_C from α4-/- mice

(right lane) were used as controls. (B) FACS immunosorting of α4+ cells from ICF_C (n=3 mice).

(C) The α4+ population from *B* was separated using an anti-CD4+ Ab (n=3 mice). (D)

Immunocytochemical detection of α4 nAChR (green), CD4 (red), and CD3 (blue) within the

ICF_C. Fluorescent signals are overlaid on DIC images. The diagram shows the proportion of

stained cells in the CD3+ ICF_C (n=3 mice). Scale bar: 50 μm. (E) A coomassie stained gel

showing the position of bands (blue boxes) analyzed by LC-ESI MS within α4 nAChR and

Gprin1 IP experiments from ICF_C. α4-/- ICF and IgG Abs were used as a negative control for the

IP. MS results are presented in Supplementary Table 2-3. Western blot confirmation of the

interaction is shown in red boxes (n=3 mice). (F) Colocalization of α4 nAChRs and Gprin1 and

phalloidin (red) in a CD4+ cell isolated using the bead assay. Bottom image: shows expression

of the proteins in actin rich domains (arrow). Scale bar: 1 μm.

FIGURE 2. Sustained nicotine promotes immune cell proliferation via the α4 nAChR. (A)

Western blot detection of α4, Gprin1, CD4, and GAPDH in the ICF. Each lane was loaded with

100 micrograms of protein (n=3 mice). (B) Changes in spleen weight in WT and α4-/- mice

injected with 0.5 or 1.0 mg/kg nicotine daily for 6 days or vehicle (Saline) (n=3 mice for WT and

α4-/-). (C) Total counted cells in ICF_C and ICF_s of nicotine treated mice (n=3 mice/condition for

WT and α4-/-). (D) FACS separation of the ICF from nicotine and saline treated mice (n=3

mice/condition for WT and α4-/-). A bead assay was used to isolate α4+ and CD3+ cells (red)

prior to FACS analysis with an anti-CD4 Ab.

FIGURE 3. Nicotine promotes proliferation of α4+CD4+Gprin1+ cells in the spleen. (A)

Immunohistochemical analysis of α4 nAChRs (green), Gprin1 (red), and CD4 (blue) in spleen

(n=3 mice). α4, Gprin1, CD16, and CD4 expressing cells were quantified in the WP and RP

regions. Triple immunolabeling (arrow) was seen in the WP. Scale bars: 50 μm; 5 μm (magnified

image). (B) Images of the WP immunostained as in *A*. Spleens were obtained from WT and α4-/-

mice injected with nicotine or saline for 6 days. Arrows point to α4+CD4+Gprin1+ cells. Scale

bar: 5 μm. (C) Percentage of cells expressing α4, Gprin1, and CD4 in spleen from total per 200

$μm^2$ area (n=3 mice/condition for WT and α4-/-). (D) Quantification of α4 nAChRs (green),

Gprin1 (red), and CD4 (blue) expression in cell suspension of the ICF_s from WT and α4-/- mice

treated with nicotine or saline (n=3 mice/condition for WT and α4-/-). Fluorescent signals are

overlaid over DIC image. Scale bar: 10 μm. (E) Localization of α4 nAChR (green), Gprin1 (red),

and CD4 (blue) in cells (same as *D*). Inset shows colocalization of α4 and Gprin1 in CD4+ cells.

Nicotine was found to promote α4 and Gprin1 expression at the cell surface and periphery

(arrow). Scale bar: 1 μm.

FIGURE 4. Nicotine promotes proliferation of α4+CD4+Gprin1+ cells and differentiation of

α4+CD133+Gprin1+ in the bone marrow. (A) Total counted cells in BMF of nicotine treated

mice (n=3 mice/condition for WT and α4-/-). (B) Localization of α4 nAChR (blue) and Gprin1

(green) in CD133+ (red) stem cells. (C) Percentage of cells expressing α4, Gprin1, and

CD4/CD133 from bone marrow (n=3 mice/condition for WT and α4-/-). (D) A comparison of

CD4+ *vs*. CD133+ expression in α4/Gprin1 expressing cells.

FIGURE 5. α4 nAChRs regulate proliferation via a Gprin1/Gα$_o$/CDC42 pathway. (A) Detection

and IP of α4, β2, and Gprin1 complexes in CEMss cells (n=3 mice for α4-/- and n=3 separate

experiments for CEMss). (-) lane: no Ab control. (B) Cell counts in response to nicotine

treatment or nicotine and (2μM) DhβE (n=3 separate experiments/condition). (C) Changes in T-

cell number following transfection of Gprin1, Gprin1 siRNA (pRNAT H1.1), CDC42 (pEGFP),

or treatment with 30μM MSP (n=3 separate experiments/condition). An empty pEGFP vector

was used as a transfection control. (D) Colocalization of Gprin1 and CDC42 in a CEMss cell.

Cells were also stained with rhodamine phalloidin (red). Scale bar: 1 μm. (E-G) Western blot

analysis of GTP-CDC42. Average % change in GTP-CDC42 relative to control groups (red)

(n=3 separate experiments/condition). (E) CEMss cells (T-cells) treated with nicotine or nicotine

and DhβE (n=3 separate experiments/condition). (F) ICF$_s$ from mice treated with saline or

nicotine for 6 days (n=3 separate trials/condition). (G) CEMss cells transfected with Gprin1

siRNA (pRNAT H1.1), CDC42 cDNA (pcDNA3), or an empty (pcDNA3) vector prior to drug

treatment (n=3 separate experiments/condition).

FIGURE 6. Nicotine promotes an increase in Th2 cytokines. Detection of Th1 and Th2

cytokines in the plasma of mice and the supernatant of cultured CEMss T-cells (n=3

mice/condition for WT and α4-/- and n=3 separate experiments/condition for CEMss). A

significant increase in the level of Th2 cytokines was detected in mice treated with nicotine for 6

days as well as CEMss cells exposed to a 0-120 min nicotine time course. CEMss cells were also

analyzed for Th1 and Th2 cytokine release in the presence of nicotine and (2μM) DHβE.

FIGURE 7. α4 nAChR signaling via the Gprin1/CDC42 pathway promotes IL-6 release from T-

cells. (A-B) Transfected cells were analyzed for IL-6 release via an ELISA (A) or a Western blot

(B) (n=3 separate experiments/condition). (C) Detection of IL-6 and cytoskeletal proteins in

CEMss cells. Bottom row: CEMss cells transfected with Gprin1 pcDNA3.1 1 prior to nicotine

treatment. Scale bar: 1μm. (D) The percentage of cells expressing IL-6 and relative percentage of

the signal within T cells (indicated ROI in *C*) (n=3 separate experiments/condition).

FIGURE 8. Nicotine's effect on immunity via the α4 nAChR signaling pathway in T-cells.

Activation of α4 nAChRs by nicotine (or ACh) engages Gprin1 leading to an inhibition of $G\alpha_o$

and CDC42 (CDC42-GDP) in T-cells. CDC42 regulates cytokine synthesis and release via the

activation of the transcription factor NFκB (Hobert et al., 2002) and the actin depolymerizing

protein cofilin (Muller et al., 2006), respectively. This nAChR pathway may serve to regulate T-
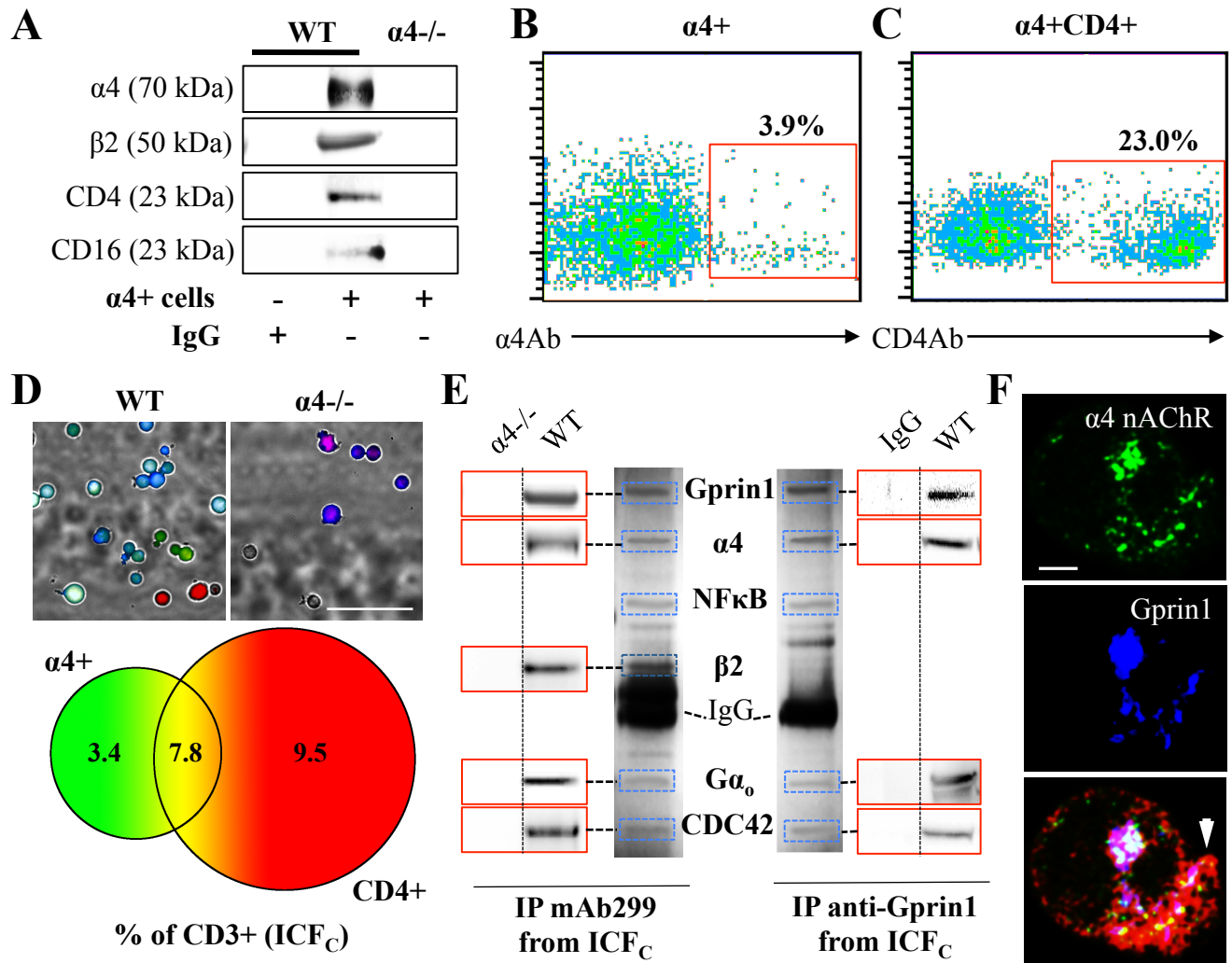
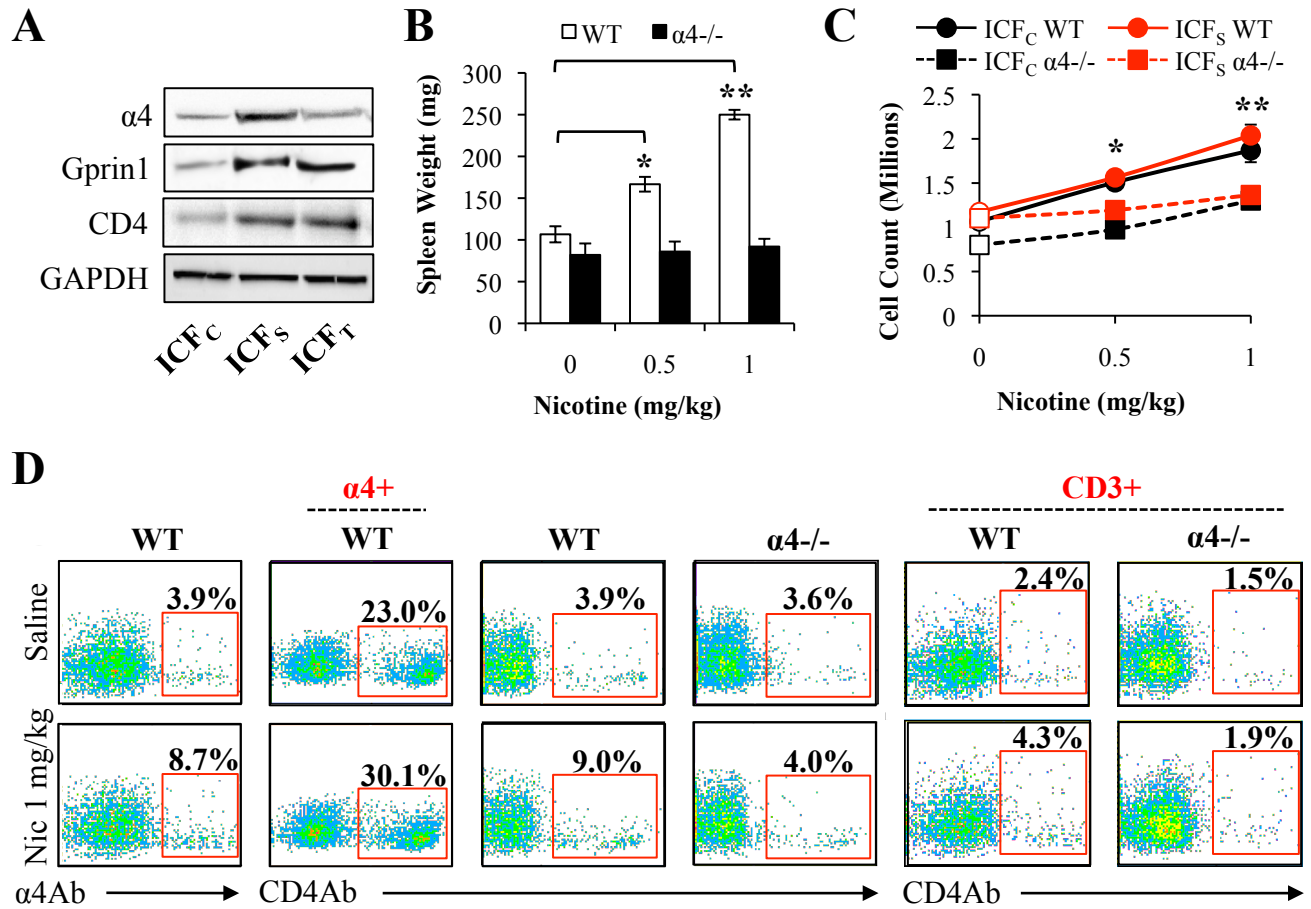cell proliferation and Th2 cytokine release.

Figure 1

A

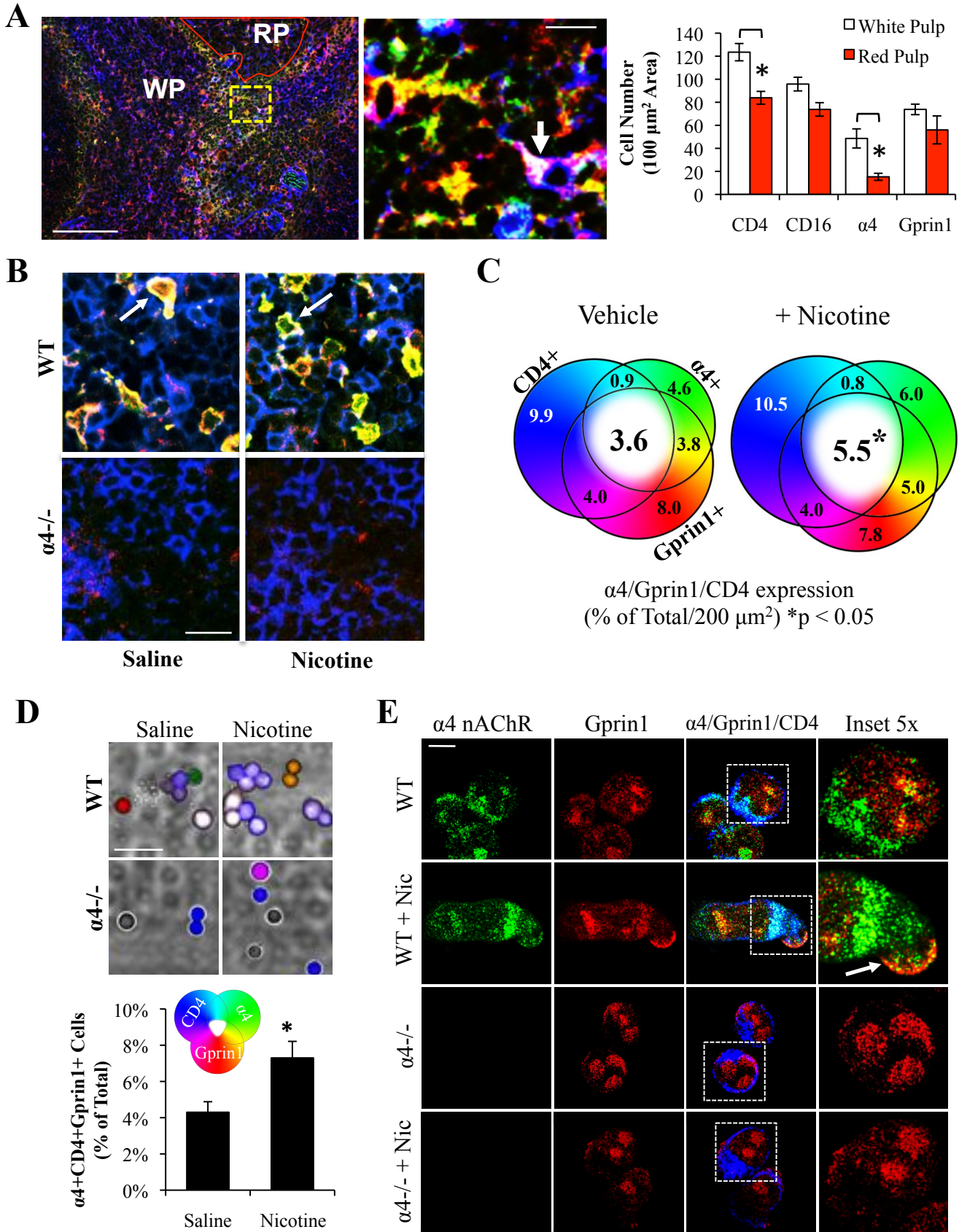|	WT	α4-/-
α4 (70 kDa)		
β2 (50 kDa)		
CD4 (23 kDa)		
CD16 (23 kDa)		
α4+ cells	- +	+
IgG	+ -	-

B α4+

3.9%

α4Ab →

C α4+CD4+

23.0%

CD4Ab →

D

WT   α4-/-

α4+ 3.4 7.8 9.5 CD4+

% of CD3+ (ICF$_C$)

E

α4-/- WT

Gprin1
α4
NFκB
β2
IgG
Gα$_o$
CDC42

IgG WT

IP mAb299 from ICF$_C$ IP anti-Gprin1 from ICF$_C$

F

α4 nAChR

Gprin1

Figure 2

Figure 3

A

WP   RP

CD4   CD16   α4   Gprin1

Cell Number (100 μm² Area)

☐ White Pulp   ■ Red Pulp

B

WT

α4-/-

Saline   Nicotine

C

Vehicle   + Nicotine

CD4+   α4+   CD4+   α4+
9.9   0.9   4.6   10.5   0.8   6.0
        3.6   5.5*
4.0   8.0   3.8   4.0   7.8   5.0
     Gprin1+

α4/Gprin1/CD4 expression
(% of Total/200 μm²) *p < 0.05

D

Saline   Nicotine

WT

α4-/-

CD4   α4
Gprin1

α4+CD4+Gprin1+ Cells (% of Total)

Saline   Nicotine

E

α4 nAChR   Gprin1   α4/Gprin1/CD4   Inset 5x

WT

WT + Nic

α4-/-

α4-/- + Nic

Figure 4

A

B

C

D

Figure 5

Figure 6

Plasma

□ WT ■ α4-/-

T-cells

○ Control ● Nic 50μM ● Nic 50μM+DHβE 2μM

Figure 7

A

+ 50μM Nicotine

IL-6 (pg/ml)

pEGFP | pEGFP | Gprin1 pcDNA3.1 | Gprin1 siRNA | CDC42 pEGFP

B

pcDNA3 | Gprin1 siRNA | CDC42 pcDNA3

IL-6

GAPDH

Nic 50μM − + + − − + − +
DHβE 2μM − − +

IL-6 O.D. (% Control)

■ Nic
□ Nic+DHβE
▦ Vehicle

Gprin1 siRNA | CDC42 pcDNA3

C

IL-6 | β-Tubulin | Phalloidin | Merge

Control

+Nicotine

+DHβE

Gprin1 pcDNA3.1

D

% Cells with IL-6 Vesicles

+Gprin1 pcDNA3.1

Nic (50μM) − + + +
DHβE (2μM) − − + −

IL-6 Signal (% Control)

+Gprin1 pcDNA3.1

Figure 8